Journal of Microbiology, Immunology and Infection (2019) 52, 90–99

Available online at www.sciencedirect.com

ScienceDirect

journal homepage: www.e-jmii.com

Original Article

Deep sequencing profiles MicroRNAs related to *Aspergillus fumigatus* infection in lung tissues of mice

Fei Chen, Xiao-yong Xu, Ming Zhang, Chen Chen, Hong-tao Shao*, Yi Shi **

Department of Respiratory and Critical Care Medicine, Nanjing General Hospital of Nanjing Military Command, Nanjing 210002, China

Received 13 January 2016; received in revised form 2 August 2016; accepted 7 September 2016
Available online 22 June 2017

KEYWORDS
Invasive pulmonary aspergillosis;
Mice;
Small RNA deep sequencing;
MicroRNA

Abstract *Background:* Invasive pulmonary aspergillosis (IPA) is a severe opportunistic infection with high mortality in patients with compromised immunity. The full repertoire of microRNAs (miRNAs) involved in the regulation of IPA infection remains to be established.
Methods: We established a mouse IPA model and analyzed small RNA transcriptomes in lung tissues of immunodeficient IPA mice (IPA group) and matched immunodeficient control mice (control group) through next-generation sequencing.
Results: A total of 3759 known miRNAs were detected, in which 23 miRNAs were identified to be related to IPA. IPA-associated miRNAs include upregulated mmu-let-7b-3p, mmu-miR124-3p, mmu-miR21a-3p, mmu-miR29c-5p, mmu-miR3473b and mmu-miR3473e, and downregulated mmu-miR-150-3p and mmu-miR-503-5p. The expression levels of eight identified miRNAs were quantified in a validation cohort ($n = 40$) by qRT-PCR, and results revealed the same change patterns. MiRNA target prediction revealed that all IPA-related miRNAs possibly engage a cooperative regulation of key elements in the NF-kappa B signaling pathway.
Conclusion: We conclude that deep-sequencing small RNAs can uncover miRNA pool-regulating IPA. Our results may lead to further understanding IPA pathogenesis and gain insight into the complexity and diversity of small RNA molecules that regulate immunodeficient IPA.

* Corresponding author. Fax: +86 25 8086 0148.
** Corresponding author. Fax: +86 25 8086 0148.
E-mail addresses: shaohongtao@126.com (H.-t. Shao), shiyi56@126.com (Y. Shi).

http://dx.doi.org/10.1016/j.jmii.2016.09.002

Introduction

Invasive pulmonary aspergillosis (IPA) is a severe opportunistic infection with high mortality, which commonly occurs in immunosuppressed patients who are old or critical ill with acquired immune deficiency syndrome (AIDS) or tuberculosis, or received allogeneic stem cell transplantation, intensive chemotherapy or solid organ transplantation. IPA incidence and mortality continuously increase in China. For instance, infection with *Aspergillus fumigatus* (*A. fumigatus*) in patients with hematologic malignancies has increased from 0.9% to 2.9% between 1989 and 2003, and mortality was as high as 79.2%—82.0%.[1—3]

MicroRNAs (miRNAs) are small regulatory RNAs of 21—24 nucleotides in length. MiRNAs degrade the target mRNA or suppress protein translation to regulate the final level of protein through sequence-specific interactions with the 3'untranslated regions (UTRs) of target genes.[4,5] MiRNA-mediated regulation covers a broad spectrum of biological processes including development, immunity and neuronal function. Cellular miRNAs are often transcribed from a DNA template located in the 5′UTRs of genes. Approximately 500 gene encoding miRNAs have been identified in mammals, and the expression of miRNAs is subject to both temporal and spatial regulation, as well as the maturing process. An initially transcribed miRNA is referred as a primary miRNA (pri-miRNA). Majority of pri-miRNAs are further processed in the nucleus by the microprocessor complex to release hairpin structured pre-miRNAs. Then, these pre-miRNAs are exported into the cytoplasm where they are further processed by Dicer and subsequently loaded onto the RNA-induced silencing complex (RISC). Once matured, miRNAs specifically bind to the 3′UTRs of the cellular mRNA target, leading to either mRNA degradation or translation inhibition.[6]

Studies have revealed that miRNA-mediated regulation is required for maintaining the normal functions of a cell, organ or body. A large number of researches have shed light on the involvement of miRNAs in various pathological processes including infectious diseases.[7,8] For instance, miRNA-155 was suggested to be essential for the T cell-mediated control of *Helicobacter pylori* infection and for the pathogenesis of chronic gastritis and colitis.[9] MiR-29a appeared to be a marker, indicating active pulmonary tuberculosis infection.[8] Both miRNA-146 and miRNA-155 were upregulated in mouse macrophages that had taken up heat-killed *Candida albicans* to modulate macrophage functions.[10] However, the possible regulation by miRNAs in IPA remains to be determined.

In an effort to gain further insight into the participation of miRNAs in IPA, the sequencing of small RNA transcriptomes isolated from lung tissues of immunodeficient IPA mice were analyzed by comparing the expression of miRNAs in matched immunodeficient control mice. Our results provide a comprehensive view of the miRNA transcriptome in a mouse model of immunodeficient IPA. Furthermore, we have identified a set of 24 miRNAs that are likely involved in the pathogenesis of IPA.

Materials and methods

Mice

Eight-to 10 week-old female C57BL/6 mice weighing 20—25 g were purchased from the Comparative Medicine Center of Nanjing University. Animal studies were reviewed and approved by Nanjing General Hospital of Nanjing Military Region under study license number scxk (SU) 2011-0003. All mice were comfortably caged in a clean room with controlled temperature and ventilation.

Preparation of *A. fumigatus* conidia

A clinical isolate of *A. fumigatus* was grown on potato dextrose agar for 5—7 days at 37 °C. Conidia were harvested by washing the culture flask with 50 ml of sterile phosphate buffered saline supplemented with 0.1% Tween 20. Then, conidia were filtered through a sterile 40-μm nylon membrane to remove hyphal fragments and enumerated with a hemacytometer.

In vivo A. fumigatus challenge, tissue burden assessment and histology

The destruction of neutrophil cells

Neutropenia (polymorphonuclear leukocytes $<100/mm^3$) was induced in mice by intraperitoneal injection of cyclophosphamide (250 mg/kg of body weight; Nanjing General Hospital of Nanjing Military Region, Nam-word [2011] B01019) on days three and one prior to inoculation. Absolute white blood cells and neutrophil counts were monitored daily throughout the study period by a Coulter counter and peripheral blood smears, respectively.

Inoculation

Mice were intratracheally administered with 8×10^6 of *Aspergillus fumigates* conidia in a volume of 25 μl under light anesthesia of chloral hydrate (Nam-word [2011] B01019). Survival of mice was monitored every 6 h post—inoculation of *A. fumigatus*.

Lung histology and staining

Left lungs were collected, fixed in 4% formalin, and paraffin-embedded. Sections were stained. Images were photographed using a Nikon Eclipse 90i microscope and Nikon NIS-Elements imaging analysis software.

RNA extraction

All lung tissues dissected for RNA analysis were preserved in RNAlater (Ambion) at −20 °C. Total RNA was extracted from lung tissues using the TRI-Reagent (Ambion). Contaminant DNA was eliminated by the addition of TURBO™ DNase (Ambion), followed by a separation step with phenol/chloroform. The quantity and quality of the extracted RNA were evaluated in the Nanodrop 1000 (Thermo Scientific) and in the 2100 Bioanalyzer (Agilent Technologies).

Lung fungal burden

Three mice were sacrificed daily, and all lungs were collected and homogenized in 1 ml of PBS to determine the lung fungal burden. Total RNA was extracted from 0.1 ml of unclarified lung homogenate using the MasterPure™ yeast RNA purification kit (Epicentre Biotechnologies, Madison, WI).[11] *A. fumigatus* burden in the lung was analyzed by real-time PCR using the *A. fumigatus* 18S rRNA (GenBank accession number AB008401)[12]; in which standard curves of *A. fumigatus* conidia (10^1–10^9) were included, as previously described.[13] Heat-killed *A. fumigatus* that were unable to grow on potato dextrose agar plates were used as negative control. No reverse transcriptase included in the cDNA reaction was used to monitor potential DNA contamination in the isolated RNA.

Small RNA library preparation and sequencing

Small RNAs ranged between 18 and 30 nt, and were ligated to the 3′ and 5′ ends of adaptors. The ligated products were reversely transcribed and amplified for 16 cycles using the adaptor primers. Resultant 150-bp fragments were isolated from PAGE. Libraries were sequenced on an Illumina HiSeq 2000 platform (Illumina, San Diego, CA). Then, the sequence image files were converted into digital-quality data.

Sequences were trimmed at both ends to remove adaptors, low quality tags were filtered out, and contaminations were eliminated. Clean reads were mapped using the SOAP software (http://soap.genomics.org.cn). Non-coding RNAs of rRNA, scRNA, snoRNA, snRNA and tRNA were first filtered using the Genbank and Rfam database; and the remaining sequencing reads were analyzed by matching exons and introns of mRNAs to locate them. Next, small RNAs were aligned to the miRNA precursors of *Homo sapiens* (miRBase release version 17) to obtain the miRNA counts. Differentially expressed miRNAs between three pairs of IPA and control samples were identified by *t*-test ($P < 0.05$). Pearson's correlation distance matrix, the average-linkage method, and log2-transformed miRNA expression levels were subjected to hierarchical clustering analysis.

qRT-PCR for miRNA expression level

Total RNA from IPA lung tissues was reversely transcribed and analyzed on CFX96 (Bio-Rad), as previously described. MiRNA expression was normalized to U6 snRNA. ΔCt ($\Delta Ct = Ct_{miRNA} - Ct_{U6}$) obtained from the IPA and control groups was compared by Mann–Whitney non-parametric statistical test. Primer sequences are listed in Table 1.

Prediction of IPA-related miRNA target genes and common pathways

The RNAhybrid software was used for predicting the target genes of the identified miRNAs. The comparison focused on the seed sequence, which is the sequence located between nucleotide two and eight from the 5′ end of the miRNA; and mismatch was not allowed (G-U pairing allowed, but no more than three). A combination of Kyoto Encyclopedia of Genes and Genomes (KEGG) and Gene Ontology (GO) was applied to identify target genes of the identified IPA-related miRNAs. Finally, focus was given on a specific pathway ID and individual KEGG pathway to pinpoint a putative gene target.

Table 1 Primer sequences.

Symbol	Primer sequence
U6	L: 5′-gcaaattcgtgaagcgttcc-3′
	R: 5′-gtgcagggtccgaggt-3′
mmu-let-7b-3p	L: 5′-cgcgcctatacaacctactgc-3′
	R: 5′-gtgcagggtccgaggt-3′
mmu-miR-124-3p	L: 5′-tgcggtaaggcacgcggtg-3′
	R: 5′-gtgcagggtccgaggt-3′
mmu-miR-21a-3p	L: 5′-gccccaacagcagtcgatg-3′
	R: 5′-gtgcagggtccgaggt-3′
mmu-miR-29c-5p	L: 5′-tgcggtgaccgatttctcctg-3′
	R: 5′-gtgcagggtccgaggt-3′
mmu-miR-3473b	L: 5′-cgcgcgggctggagagatggctcag-3′
	R: 5′-cccacgtccgtagaaaggta-3′
mmu-miR-3473e	L: 5′- tgcgggggctggagagatggctcgta-3′
	R: 5′-gtgcagggtccgaggt-3′
mmu-miR-150-3p	L: 5′-gcccctggtacaggcctg-3′
	R: 5′-gtgcagggtccgaggt-3′
mmu-miR-503-5p	L: 5′-tgcggtagcagcgggaacag-3′
	R: 5′-gtgcagggtccgaggt-3′

Statistical analysis

Survival percentages were analyzed over time and survival curves were drawn using SPSS 17 statistical software. All quantitative data were analyzed by X ± standard deviation (SD). The difference between groups was analyzed by analysis of variance, while survival time was analyzed by log-rank Mantel–Cox test. The difference was statistically significant when *P* was <0.05.

Results

Neutropenia and IPA mouse model

Neutrophil deficiency/dysfunction is a critical factor facilitating invasive pulmonary aspergillosis.[14,15] In order to verify neutropenic mice, neutrophil counts were monitored every 24 h (q24 h) throughout the study period with a Coulter counter and peripheral blood smears, respectively. Neutrophil counts constantly remained below 100/mm^3 during the experiment (Table 2). From the day of infection up to day four post-infection, the number of neutrophils were consistently lower than 100/μl; which was significantly lower in the IPA group (intratracheally with 8×10^6 conidia at a volume of 25 μl) and met the criteria of compromised immunity, compared with the normal group (no intervention) and PBS group (intratracheally with 25 μl of PBS) ($P < 0.05$).

Neutropenic mice were intraperitoneally infected with 8×10^6 of *A. fumigates* conidia or PBS in a volume of 25 μl. More than 70% of IPA mice died on day three post-infection, while all of them survived in the PBS group (Figure 1A). Real-time PCR detection of *A. fumigatus* 18S rRNA in lung

Table 2 The number of peripheral blood neutrophils in mice after cyclophosphamide injection (neutrophils/μl).

Group	n	0d	1d	2d	3d	4d
Normal	5	658 ± 93				
IPA[a]	5	89 ± 12	73 ± 12	68 ± 9	65 ± 8	73 ± 6
PBS[b]	5	83 ± 5	65 ± 14	69 ± 14	75 ± 7	87 ± 9

[a] IPA group *vs.* normal group, $P < 0.05$.
[b] PBS group *vs.* normal group, $P < 0.05$.

tissue, the most sensitive method for determining lung fungal burden in experimental aspergillosis,[16] revealed the highest *A. fumigatus* burden in IPA mice at day one post-infection. The *A. fumigatus* burden was gradually reduced over time. However, the *A. fumigatus* burden in IPA mice remained significantly higher than PBS mice ($P < 0.05$), as shown in Figure 1B.

Changes in *A. fumigatus* invasion and lung histology in neutropenia IPA mice

Gross (Figure 2A) and micro-pathology (Figure 2B) in lungs were observed in IPA mice. Lung tissues in the PBS group were pink, and became dark in the IPA group. Visible hemorrhage and white nodules gradually increased in the IPA group, where white nodules represent *A. fumigatus* infection foci.

Lung hematoxylin and eosin sections revealed profound and intense pathological changes in IPA mice (Figure 2B). Vascular congestion, edema, inflammatory cell infiltration, and alveolar hemorrhage gradually became severe; and normal alveolar structure progressively disappeared after infection.

Deep sequencing of small RNAs isolated from lung tissues of IAP mice

Three IPA mice lung tissues were collected at day three post-infection (assigned as 25-3d, 26-3d and 27-3d), and three lung tissues (pooled together, assigned as 1-0d) of neutropenic mice prior to infection were selected for deep sequencing of miRNAs. More than a million high-quality reads were generated from deep sequencing, and majority of the sequences were 21—23 nucleotides long (Figure 3). More than 90% of clean reads were retained after filtering out low-quality tags, removing adaptors and cleaning up contaminations (Table 3). Small RNA sequence types (represented by uniqueness) and length distribution were analyzed. The total number of unique clean reads from the small RNA libraries of the IPA and control groups was 261,009 and 967,604, respectively. After comparing these small RNA sequences with the NCBI Genbank and Rfam database (requirements between two databases priority Genbank > Rfam), 1,215,154 reads of rRNA, tRNA, snRNA, snoRNA and repeat-associated small RNAs were annotated and removed (Figure 4). The remaining 14,460 unique sequences were retained for miRNA analysis, consisting of 10,991 from IPA mice and 3468 from the control group, respectively. The predicted miRNA candidates were mainly obtained by targeting miRNA biometric screening and the miRNA prediction software (Mireap; http://sourceforge.net/projects/mireap/).

Correlative analysis of miRNA expression profiles

In order to compare miRNA expression profiles between the three pairs of IPA and PBS mice, pairwise comparisons and correlative analysis were performed. The scatter plot of log2-ratio was used to express the miRNAs in the two samples, as shown in Figure 5. A total of 58 conserved miRNAs were differently expressed ($P < 0.05$) between 25-3d and 1-0d, in which the expression of 28 miRNAs were upregulated and the expression of 30 miRNAs were downregulated. In comparing 26-3d with 1-0d, we found that 89 conserved miRNAs were differently expressed ($P < 0.05$), in which the expression of 43 miRNAs were upregulated and the expression of 46 miRNAs were downregulated. Furthermore, we found that 102 conserved miRNAs were differently expressed ($P < 0.05$), in which the expression in

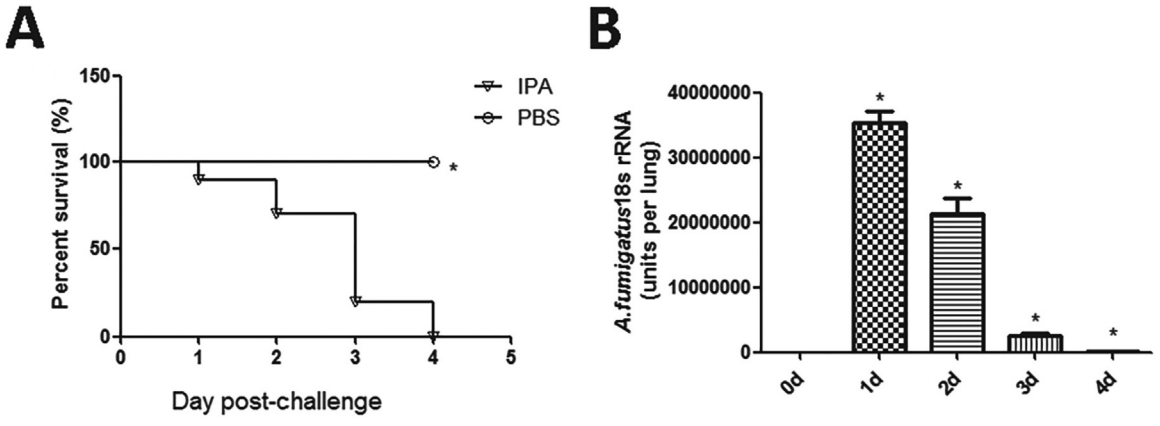

Figure 1. Neutropenia and IPA mouse model. (A) Neutropenic mice were intratracheally inoculated with 8×10^6 conidia or PBS in a volume of 25 μl, and survival was monitored for four days; *$P < 0.05$ (log-rank Mantel—Cox test). **(B)** Real-time PCR analysis of *Aspergillus fumigatus* (*A. fumigatus*) 18S rRNA levels in lungs of neutropenic mice challenged intratracheally with 8×10^6 conidia or PBS in a volume of 25 μl, and lung tissues were collected every 24 h post—challenge; $n = 3$ mice/group for this study. Data are expressed as the mean of *A. fumigatus* 18S rRNA levels ± SEM; *$P < 0.05$ (Unpaired two-tailed Student's test).

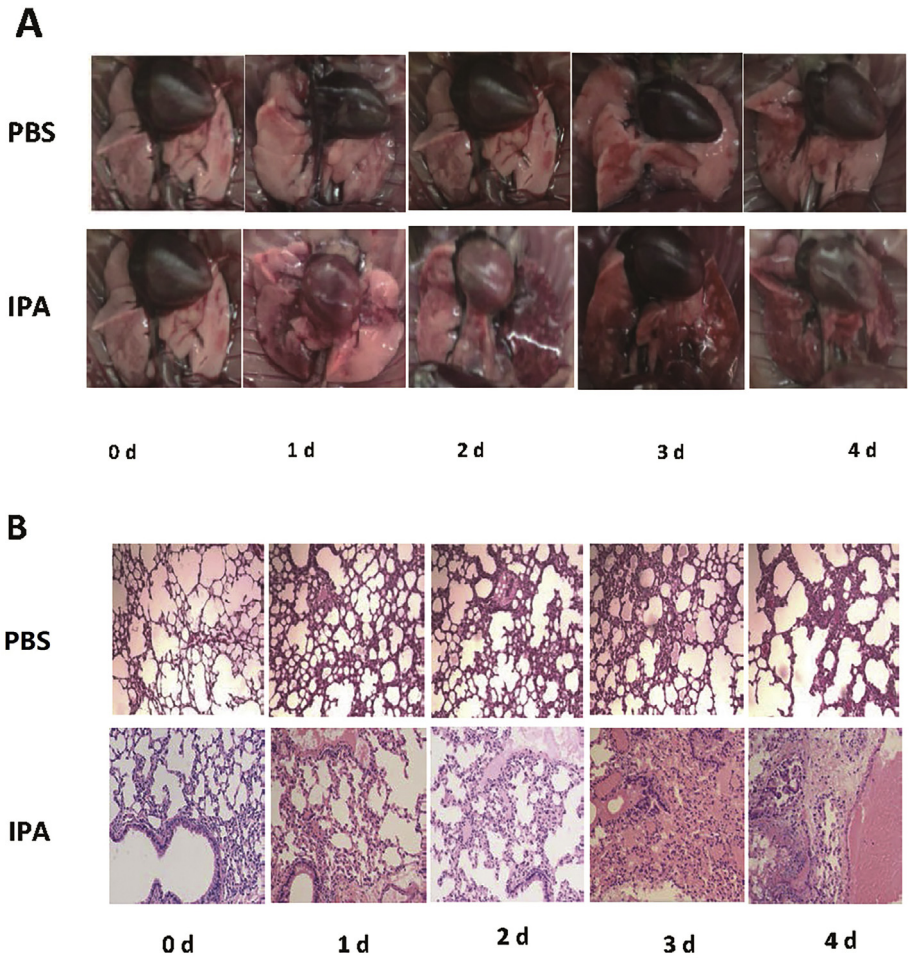

Figure 2. Changes in lung pathology in the two groups after *Aspergillus fumigatus* invasion. Neutropenic mice were challenged intratracheally with 8×10^6 conidia or PBS in a volume of 25 μl. **(A)** Representative gross lung tissue of the IPA and PBS groups monitored daily for four days post-infection. **(B)** Representative H&E-stained lung sections from IPA and PBS over five time points; original magnification, 200×; left image represents 100 μm.

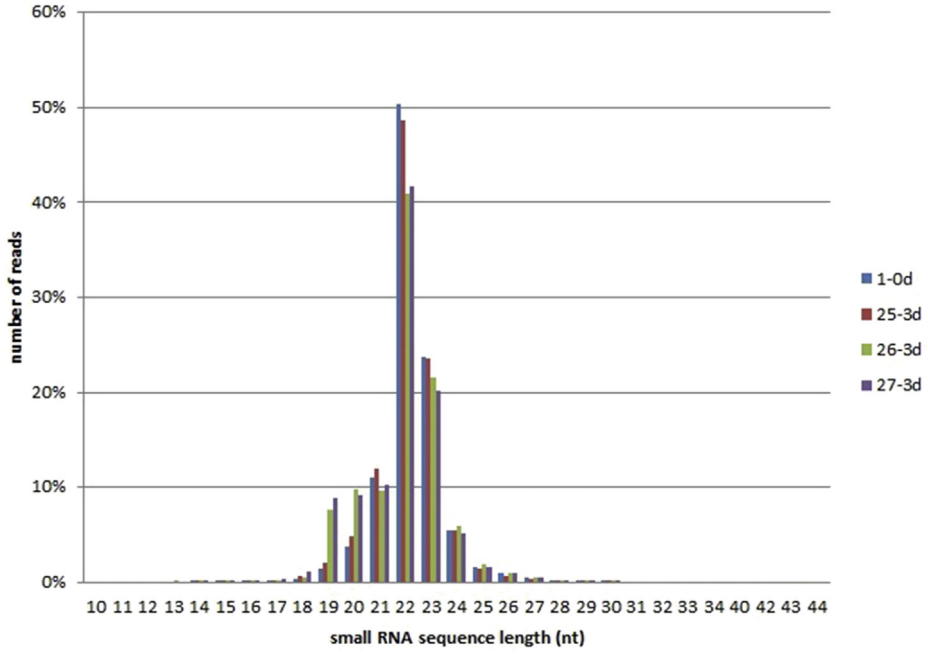

Figure 3. The length distribution of small RNAs in the IPA (forms 25-3d, 26-3d, 27-3d) and control groups (1-0d).

Table 3 Data quality of small RNAs in the IPA and control groups.

Sample List	Total reads	Clean reads	Percentage (%)
1-0d	9,571,879	9,491,589	99.48
25-3d	9,058,574	8,973,384	99.39
26-3d	9,712,588	9,585,198	99.02
27-3d	9,819,188	9,708,933	99.21

56 miRNAs were upregulated and the expression in 46 miRNAs were downregulated between 27-3d and 1-0d.

Variance analysis of conserved miRNA expression profiles

Variants of miRNAs, called isomiRs, are commonly reported in deep-sequencing reads. IsomiRs are derived from the same pre-miRNAs, but exhibit sequence variations from the reference miRNAs in the miRBase.[17] In this study, such sequence divergence was also observed. Results from next-generation sequencing (NGS) found heterogeneity in the sequence and length of the identified miRNAs. As shown in Table 4, 23 miRNAs were deferentially expressed between IPA and control; in which 14 miRNAs were upregulated and nine miRNAs were downregulated. The expression levels of mmu-let-7b-3p, mmu-miR124-3p, mmu-miR21a-3p, mmu-miR29c-5p, mmu-miR3473b and mmu-miR3473e were more than two-folds higher in three IPA libraries than in the control library. In contrast, mmu-miR-150-3p and mmu-miR-503-5p were downregulated for more than two-folds.

Verification of conserved miRNA expression by qRT-PCR

In order to verify the accuracy of differentially expressed miRNAs, stem-loop RT-PCR validation was performed on the total RNA isolated from control ($n = 20$) and IPA ($n = 20$) samples. Verified miRNAs that were differentially expressed for more than two-fold included six with upregulation (mmu-let-7b-3p, mmu-miR124-3p, mmu-miR21a-3p, mmu-miR29c-5p, mmu-miR3473b and mmu-miR3473e) and two with downregulation (mmu-miR-150-3p and mmu-miR-503-5p). The expression of mmu-let-7b-3p, mmu-124-3p, mmu-miR21a-3p, mmu-miR29c-5p, mmu-miR3473b, mmu-miR3473e, mmu-miR-150-3p and mmu-miR-503-5p were significantly and differently expressed between these two groups, which is consistent with sequencing results shown in Figure 6.

Prediction of target genes of identified IPA-related miRNAs

The identification of the target genes of miRNAs is required for understanding the functions of miRNAs. The predicted target genes for the differently expressed miRNAs with the described parameter in the Methods section are shown in Table 5.

We selected predicted targets that were co-transcribed with miRNAs to predict the biologic functions of the

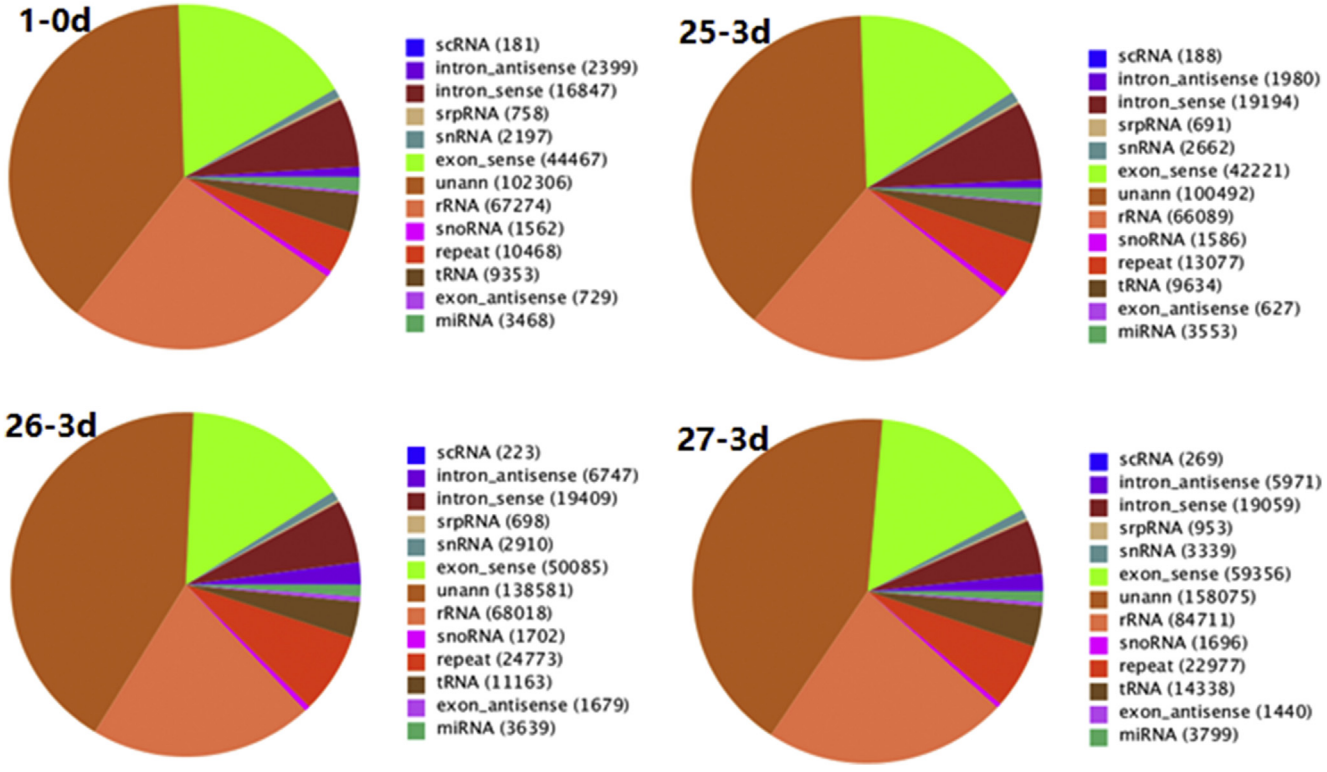

Figure 4. The distribution of different types of small RNAs in the IPA (forms 25-3d, 26-3d, 27-3d) and control groups (1-0d).

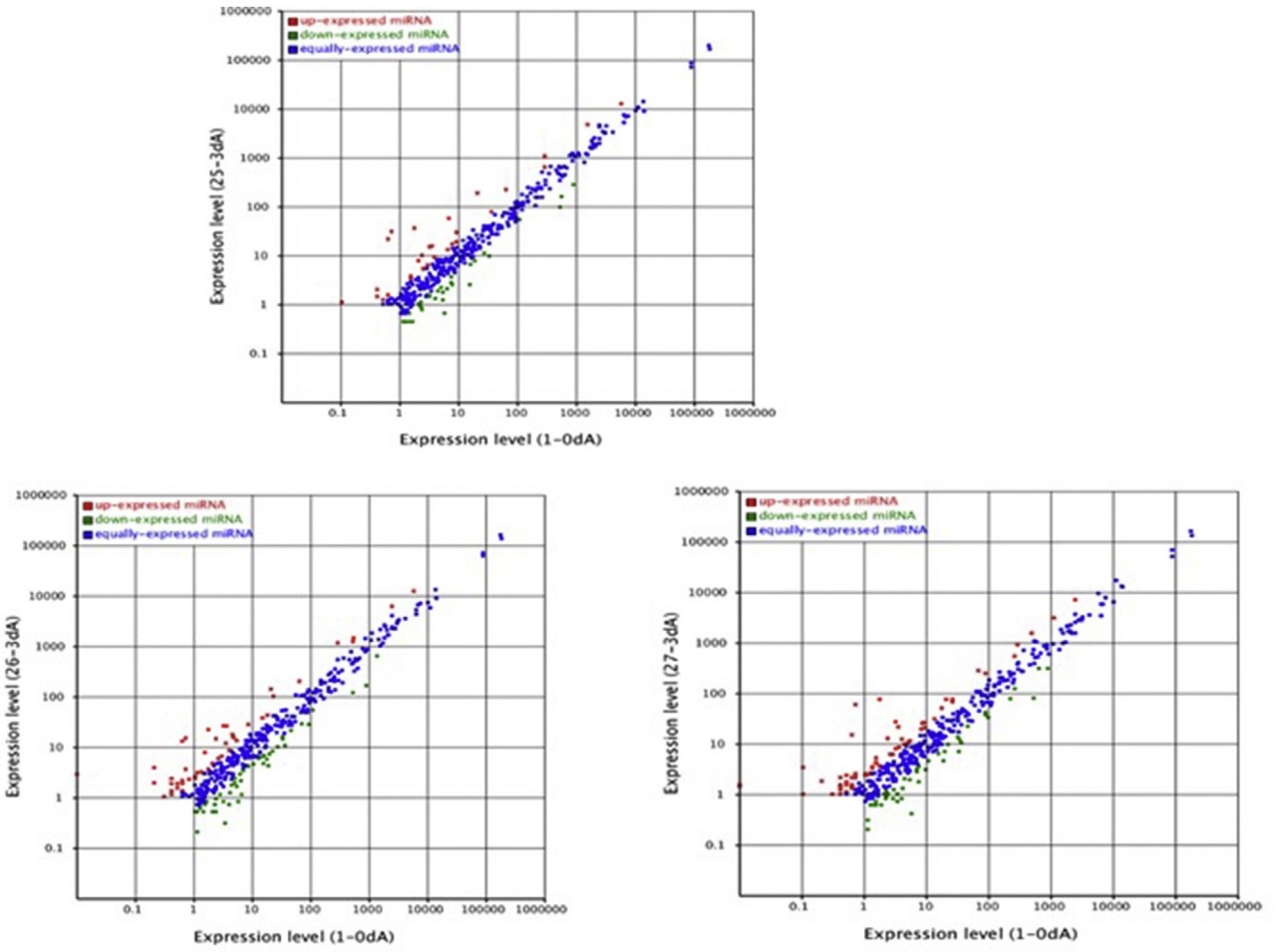

Figure 5. The scatter plot map for miRNA expression levels in the IPA and PBS groups. The expression of each miRNA was calculated by dividing the number of reads by the total number of miRNAs in the same library. Each dot represents the expression of a single miRNA in two genomic compositions. The blue dots represent the $1/2 \leq$ ratio ≤ 2 miRNAs, the red dots represent the ratio >2 miRNAs, and the green dots represent the ratio $<1/2$ between two genomic compositions (ratio = IPA/PBS).

identified miRNAs. Sequence mmu-let-7b-3p, mmu-124-3p, mmu-miR21a-3p, mmu-miR29c-5p, mmu-miR3473b and mmu-miR3473e were upregulated in 25-3d *vs.* 1-0d, 26-3d *vs.* 1-0d, and 27-3d *vs.* 1-0d; while sequence mmu-miR-150-3p and mmu-miR-503-5p were downregulated. We used KEGG and GO function annotation to identify pathways that were actively regulated by these two series of miRNAs. Analyses of each specific KEGG pathway of mmu-let-7b-3p, mmu-124-3p, mmu-miR21a-3p, mmu-miR29c-5p, mmu-miR3473b, mmu-miR3473e, mmu-miR-150-3p and mmu-miR-503-5p in IPA appeared to merge into the NF-kappa B signaling pathway. Within this pathway, more than one miRNA is often predicted to target Syk, LBP, P52, P100, TBA and BAFF; where the same gene could be potentially targeted by several co-transcribed miRNAs.

Prediction of novel miRNAs

Variance analysis of the miRNA pool revealed not only the conserved miRNAs, but also the novel miRNAs. A panel of 198 unique sequences was identified as putatively novel miRNAs. The miRNA hairpins are mostly located in intergenic regions, introns or reverse repeat of coding sequences. The characteristic hairpin structure of the miRNA precursor can be used to predict the novel miRNA. The novel miRNA was predicted by summing the count of those miRNAs with no more than three mismatches on the 5′ and 3′ ends and with no mismatch in the middle from the alignment result. Finally, we ranked the top 18 putatively novel miRNAs out of the 198 sequences. Among the 18 novel miRNAs, candidate-2 revealed a significant difference in the fold of expression when normalized to the total miRNA count and compared between the IPA and control groups (Figure 7). The sequence of candidate-2 consists of AATGTGGAAGTGGTCTGAGGCAT, which targets the P50 gene at the NF-kappa B signaling pathway.

Discussion

A. fumigatus is a common saprophyte that widely spreads on the surface of the skin and mucosa, and would not cause a disease under normal circumstances. However, when large amounts of *A. fumigatus* spores were inhaled into immunocompromised patients, IPA can occur[18]; which

Table 4 Altered expression of miRNAs in IPA lung tissue.

No.	Name	25-3d *vs.* 0d (Fold change)	26-3d *vs.* 0d (Fold change)	27-3d *vs.* 0d (Fold change)
1	mmu-let-7b-3p	2.25	2.5096	2.398
2	mmu-miR-122-5p	−1.6769	−2.4384	−1.5432
3	mmu-miR-124-3p	5.1182	4.3667	4.5624
4	mmu-miR-132-3p	3.1621	2.7554	1.8543
5	mmu-miR-142-3p	−2.6146	−1.7415	−1.2976
6	mmu-miR-150-3p	−3.11549	−2.7956	−3.8140
7	mmu-miR-150-5p	−1.7769	−1.2023	−2.2626
8	mmu-miR-218-5p	−1.5819	−2.4547	−2.2805
9	mmu-miR-21a-3p	2.2249	3.0373	3.0846
10	mmu-miR-29c-5p	2.0493	2.6120	2.3863
11	mmu-miR-331-3p	2.1331	1.7439	2.6010
12	mmu-miR-3473b	4.3378	3.6263	5.4112
13	mmu-miR-3473e	5.4132	4.3584	6.670
14	mmu-miR-351-3p	−1.2611	−2.1485	−2.0327
15	mmu-miR-383-5p	−15914	−1.6866	−1.4571
16	mmu-miR-466a-3p	−1.3784	−1.6662	−1.3221
17	mmu-miR-miR-466b-3p	−1.3784	−1.6662	−1.3221
18	mmu-miR-466c-3p	−1.3784	−1.6662	−1.3221
19	mmu-miR-466e-3p	−1.3784	−1.6662	−1.3221
20	mmu-miR-466p-3p	−1.3784	−1.6662	−1.3221
21	mmu-miR-503-5p	−2.4584	−2.447	−2.7457
22	mmu-miR-543-3p	−1.2578	−1.3529	−1.137-
23	mmu-miR-92a-1-5p	1.2616	2.3269	1.729

Positive numbers are upregulated, while negative numbers are downregulated.

usually result in approximately 80% of mortality. IPA pathogenesis is currently not well—understood, and many factors including miRNAs are likely involved, because accumulated data has shown that miRNAs regulate the response of hosts to infections of viral, bacterial and fungal pathogens.[9,19,20] The expression profile of miRNAs in lung tissues of IPA patients needs to be established before probing for possible functions and mechanisms of individual miRNAs in IPA pathogenesis. We used an IPA mouse model to achieve our goal in this study.

We first established a neutropenic mouse model by intraperitoneally injecting cyclophosphamide, and the neutrophil count was observed to constantly remain below 100/mm^3. Immunity-compromised mice became susceptible to *A. fumigatus* infection. The breathing of infected animals increased, weight loss occurred, activity decreased, and all mice died at day four post-infection. The highest fungal load was detected at day one after inoculation in infected lung tissues, which gradually reduced over time. The gross pathologic changes included gradually increased hemorrhage and white nodular lesions. Under microscopic observation, *A. fumigatus* spores germinated in lung tissues and a hyphae group was noted. These results confirmed the successful establishment of the IPA mouse model.

In order to identify which and now many miRNAs are likely involved in IPA pathogenesis, we profiled global miRNAs in lung tissues of mice from both the IPA and control groups using NGS. By comparing the expression level of

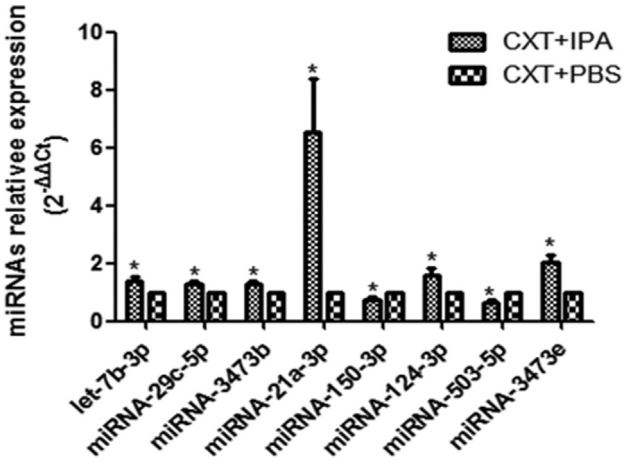

Figure 6. Validation of miRNA expression profiles by qRT-PCR. Total RNA from lung tissues in the PBS ($n = 20$) and IPA ($n = 20$) groups was analyzed, and the relative expression of miRNAs was plotted. RNA U6 was used as an internal control. Experiments were repeated three times and similar results were obtained. All results, normalized to U6 mRNA expression, were expressed as $2^{-\triangle\triangle Ct}$ ($\triangle Ct = Ct_{miRNAs} - Ct_{U6}$, $\triangle\triangle Ct = Ct_{IPA} - \triangle Ct_{PBS}$) and mean ± standard error of the mean (SEM); *, *vs.* PBS lung tissue, $P < 0.05$.

Table 5 Predicted target genes of IPA-related miRNAs.

Sample name	miRNA number	Target gene number	Location number
25-3d *vs.* 1-0d	52	1337	1735
26-3d *vs.* 1-0d	70	2432	2918
27-3d *vs.* 1-0d	88	3819	4664

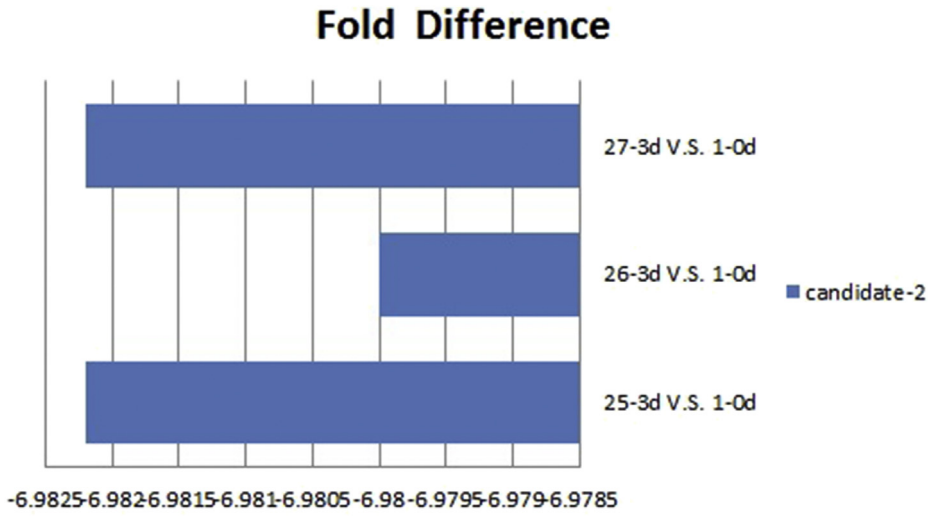

Figure 7. Predicted structures and fold differences of novel miRNAs. The fold difference in expressing candidate-2 was significantly lower in the IPA group compared to the control group.

miRNAs between IPA and controls, a panel of 23 miRNAs considered to be IPA-related was suggested; in which 14 miRNAs were upregulated and nine miRNAs were down-regulated. Furthermore, eight of 23 miRNAs were selected for further verification by expanding test samples to 20 for each group using stem-loop RT-PCR. The same changed patterns for the eight miRNAs were found, suggesting that those miRNAs were likely IPA-related. Our results provide a basis for further characterizing individual miRNAs that participate in IPA pathogenesis.

In this study, isomiRs such as mmu-let-7b-3p were notable. The isomiRs, which vary in length, are presumably the products of flexibility in cleavage positions directed by Dicer and Drosha, or of end-processing; whereas variations in the length of nucleotides are likely generated during miRNA maturation. The addition of non-template nucleotides to the 3'ends of isomiRs may contribute to miRNA stability, which is required for exercising the functions of miRNAs[17] including the involvement in the pathogenesis of many human diseases[17,21–23] and attenuation of the specific effects of some miRNAs.[24] However, the full impact of variations at the length of the miRNAs on their biological functions remains to be determined.

These eight miRNAs were mapped to a specific KEGG pathway, and the involvement of the NF-kappa B signaling pathway in IPA pathogenesis appeared prominent. More than one miRNA was predicted to target Syk, LBP, P52, P100, TBA and BAFF; and all of which are components of this pathway. A novel miRNA (candidate-2) was identified in lung tissues of both the IPA and control groups. This newly identified miRNA seemed to target the P50 gene of the NF-kappa B signaling pathway. Function annotation of the predicted target genes of the 24 IPA-related miRNAs revealed a broad range of metabolic pathways and biosynthesis processes. To our knowledge, this is the first study to profile a pool of miRNAs in lung tissues of IPA mice. Our findings support the hypothesis that miRNAs may contribute to IPA pathogenesis possibly through the regulation of their target genes.

In conclusion, we profiled a pool of miRNAs in lung tissues of IPA mice using NGS, and identified a panel of 23 miRNAs as IPA-related. Furthermore, we validated the expression profiles of eight of 23 identified miRNAs in 40 more mice lung tissues by RT-qPCR. Notably, the eight miRNAs were mapped to the NF-kappa B signaling pathway, suggesting that the participation of miRNAs in IPA pathogenesis may be mediated through the NF-kappa B signaling pathway.

Disadvantage and expectations

The host's immune response to Aspergillus is a complex biological process. Immune suppression affects the prognosis of IPA. The exact functions of miRNAs involved in IPA pathogenesis and the NF-kappa B signaling pathway have not been validated in the current study. In the future, we intend to investigate the kinetic changes of miRNA under immune suppression and explore its related signaling pathways, which would likely lay a foundation for regulating immune response.

Conflicts of interest statement

None declared.

References

1. Vandewoude K, Blot S, Benoit D, Depuydt P, Vogelaers D, Colardyn F. Invasive aspergillosis in critically ill patients: analysis of risk factors for acquisition and mortality. *Acta Clin Belg* 2004;**59**:251—7.
2. Vandewoude KH, Blot SI, Depuydt P, Benoit D, Temmerman W, Colardyn F, et al. Clinical relevance of Aspergillus isolation from respiratory tract samples in critically ill patients. *Crit Care* 2006;**10**:R31.
3. Baddley JW, Andes DR, Marr KA, Kauffman CA, Kontoyiannis DP, Ito JI, et al. Antifungal therapy and length of hospitalization in

transplant patients with invasive aspergillosis. *Med Mycol* 2013; **51**:128—35.
4. Aigner A. MicroRNAs (miRNAs) in cancer invasion and metastasis: therapeutic approaches based on metastasis-related miRNAs. *J Mol Med Berl* 2011;**89**:445—57.
5. Ambros V. The functions of animal microRNAs. *Nature* 2004; **431**:350—5.
6. Bartel DP. MicroRNAs: genomics, biogenesis, mechanism, and function. *Cell* 2004;**116**:281—97.
7. Thirion M, Ochiya T. Roles of microRNAs in the hepatitis B virus infection and related diseases. *Viruses* 2013;**5**:2690—703.
8. Fu Y, Yi Z, Wu X, Li J, Xu F. Circulating microRNAs in patients with active pulmonary tuberculosis. *J Clin Microbiol* 2011;**49**: 4246—51.
9. Oertli M, Engler DB, Kohler E, Koch M, Meyer TF, Muller A. MicroRNA-155 is essential for the T cell-mediated control of Helicobacter pylori infection and for the induction of chronic Gastritis and Colitis. *J Immunol* 2011;**187**:3578—86.
10. Monk CE, Hutvagner G, Arthur JS. Regulation of miRNA transcription in macrophages in response to Candida albicans. *PLoS One* 2010;**5**:e13669.
11. Mattila PE, Metz AE, Rapaka RR, Bauer LD, Steele C. Dectin-1 Fc targeting of aspergillus fumigatus beta-glucans augments innate defense against invasive pulmonary aspergillosis. *Antimicrob Agents Chemother* 2008;**52**:1171—2.
12. Bowman JC, Abruzzo GK, Anderson JW, Flattery AM, Gill CJ, Pikounis VB, et al. Quantitative PCR assay to measure Aspergillus fumigatus burden in a murine model of disseminated aspergillosis: demonstration of efficacy of caspofungin acetate. *Antimicrob Agents Chemother* 2001;**45**:3474—81.
13. Werner JL, Metz AE, Horn D, Schoeb TR, Hewitt MM, Schwiebert LM, et al. Requisite role for the Dectin-1 -glucan receptor in pulmonary defense against Aspergillus fumigatus. *J Immunol* 2009;**182**:4938—46.
14. Fukuda T, Boeckh M, Carter RA, Sandmaier BM, Maris MB, Maloney DG, et al. Risks and outcomes of invasive fungal infections in recipients of allogeneic hematopoietic stem cell transplants after nonmyeloablative conditioning. *Blood* 2003; **102**:827—33.
15. Barnes PD, Marr KA. Risks, diagnosis and outcomes of invasive fungal infections in haematopoietic stem cell transplant recipients. *Br J Haematol* 2007;**139**:519—31.
16. Sheppard DC, Marr KA, Fredricks DN, Chiang LY, Doedt T, Filler SG. Comparison of three methodologies for the determination of pulmonary fungal burden in experimental murine aspergillosis. *Clin Microbiol Infect* 2006;**12**:376—80.
17. Fernandez-Valverde SL, Taft RJ, Mattick JS. Dynamic isomiR regulation in Drosophila development. *RNA* 2010;**16**:1881—8.
18. Romani L. Immunity to fungal infections. *Nat Rev Immunol* 2011;**11**:275—88.
19. Shwetha S, Gouthamchandra K, Chandra M, Ravishankar B, Khaja MN, Das S. Circulating miRNA profile in HCV infected serum: novel insight into pathogenesis. *Sci Rep* 2013;**3**: 1555.
20. Navarro L, Dunoyer P, Jay F, Arnold B, Dharmasiri N, Estelle M, et al. A plant miRNA contributes to antibacterial resistance by repressing auxin signaling. *Science* 2006;**312**:436—9.
21. Guo L, Yang Q, Lu J, Li H, Ge Q, Gu W, et al. A comprehensive survey of miRNA repertoire and 3' addition events in the placentas of patients with pre-eclampsia from high-throughput sequencing. *PLoS One* 2011;**6**:e21072.
22. Vaz C, Ahmad HM, Bharti R, Pandey P, Kumar L, Kulshreshtha R, et al. Analysis of the microRNA transcriptome and expression of different isomiRs in human peripheral blood mononuclear cells. *BMC Res Notes* 2013;**6**:390.
23. McGahon MK, Yarham JM, Daly A, Guduric-Fuchs J, Ferguson LJ, Simpson DA, et al. Distinctive profile of IsomiR expression and novel microRNAs in rat heart left ventricle. *PLoS One* 2013;**8**:e65809.
24. Burroughs AM, Ando Y, de Hoon MJ, Tomaru Y, Nishibu T, Ukekawa R, et al. A comprehensive survey of 3' animal miRNA modification events and a possible role for 3' adenylation in modulating miRNA targeting effectiveness. *Genome Res* 2010; **20**:1398—410.